Journal of Power Sources 195 (2010) 5379–5381

Contents lists available at ScienceDirect

Journal of Power Sources

journal homepage: www.elsevier.com/locate/jpowsour

Short communication

Fe_3O_4 submicron spheroids as anode materials for lithium-ion batteries with stable and high electrochemical performance

Suqing Wang, Jingying Zhang, Chunhua Chen*

CAS Key Laboratory of Materials for Energy Conversion, Department of Materials Science and Engineering, University of Science and Technology of China, Hefei, Anhui 230026, China

ARTICLE INFO

Article history:
Received 7 October 2009
Received in revised form 23 January 2010
Accepted 9 March 2010
Available online 15 March 2010

Keywords:
Magnetite
Microsphere
Hydrothermal
Lithium battery
Electrode

ABSTRACT

A magnetite (Fe_3O_4) powder composed of uniform sub-micrometer spherical particles has been successfully synthesized by a hydrothermal method at low temperature. X-ray diffraction, scanning electron microscopy, transmission electron microscopy and galvanostatic cell cycling are employed to characterize the structure and electrochemical performance of the as-prepared Fe_3O_4 spheroids. The magnetite shows a stable and reversible capacity of over 900 mAh g^{-1} during up to 60 cycles and good rate capability. The experimental results suggest that the Fe_3O_4 synthesized by this method is a promising anode material for high energy-density lithium-ion batteries.

© 2010 Elsevier B.V. All rights reserved.

1. Introduction

Transition metal oxides (MO, M = Cu, Fe, Co, etc.) as a new series of anode materials for lithium-ion batteries can reach markedly higher specific capacity of more than 600 mAh g^{-1} compared with that of graphite (372 mAh g^{-1}) [1]. In the past decades, the magnetite Fe_3O_4 has been widely investigated for many fields, such as ferromagnetic, biomedical, and catalysis applications [2,3]. It is also interesting to be used in lithium-ion batteries as an anode material with a very high theoretical capacity of 928 mAh g^{-1} [1,4]. It is now well accepted that the limitations in the rate capability of lithium-ion batteries are mainly caused by the slow diffusion of lithium ions in the electrode materials [5]. In order to improve the capability of Fe_3O_4, many approaches have been used in the literature, such as carbon-coating, nanocomposite, and nanostructure [6–9]. Wexler et al. have fabricated magnetite/carbon core–shell nanorods electrodes which can supply reversible capacity of 600 mAh g^{-1} (~400 mAh g^{-1} after 100th cycle) [6]. Guo et al. have synthesized Fe_3O_4 nanocrystals @C composite that can exhibit 600 mAh g^{-1} (around 30 cycles) [10]. Wan et al. have developed a carbon-coated magnetite that can deliver a reversible capacity of 530 mAh g^{-1} at *C*/2 rate (up to 80 cycles) [11]. Kim et al. have demonstrated that Fe/Fe_3O_4 core–shell nanostructure electrodes can release a reversible capacity of about 600 mAh g^{-1} after 50 cycles [12].

In this paper, we have synthesized uniform submicron spheroids of magnetite by a low-temperature hydrothermal method. The submicron spheres are self-assembled with many 30 nm nanospheres and nano-pores which can provide large surface area. When used as an electrode material, they can tolerate volume change during the charge/discharge process which secures a highly stable and reversible capacity of over 900 mAh g^{-1}, which value is greater than that of Fe_3O_4 films or carbon-coated Fe_3O_4 reported before (700 mAh g^{-1}) [6,7,10–13]. Due also to its nanostructure, it also exhibits very high rate capability.

2. Experimental details

Fe_3O_4 sub-microsphere was synthesized through a hydrothermal method [14]. $FeCl_3 \cdot 6H_2O$ (1.35 g) was dissolved in ethylene glycol (15 ml) to form a clear yellow solution A. Sodium acetate (NaAc, 3.6 g) and polyethylene glycol (PEG2000, 1 g) were dissolved in ethylene glycol (20 ml) to form a transparent solution B. Then solution B was added dropwise into solution A with stirring to produce some yellowish precipitate. After a vigorous stirring for 10 min, the suspension was sealed in a teflonlined stainless-steel autoclave (50 ml capacity). The autoclave was heated to and maintained at 200 °C for 48 h, and then allowed to cool to room temperature to convert the yellowish precipitate into a black solid product. It was washed by deionized water and ethanol for several times, and then was vacuum-dried at 70 °C for 12 h.

The crystalline structure and particle morphology of this black solid were characterized by X-ray diffraction (XRD) (Philips X'Pert PRO SUPER, Cu Kα radiation, λ = 1.5406 nm), scanning electron

* Corresponding author. Tel.: +86 551 3606971; fax: +86 551 3601592.
E-mail address: cchchen@ustc.edu.cn (C. Chen).

0378-7753/$ – see front matter © 2010 Elsevier B.V. All rights reserved.
doi:10.1016/j.jpowsour.2010.03.035

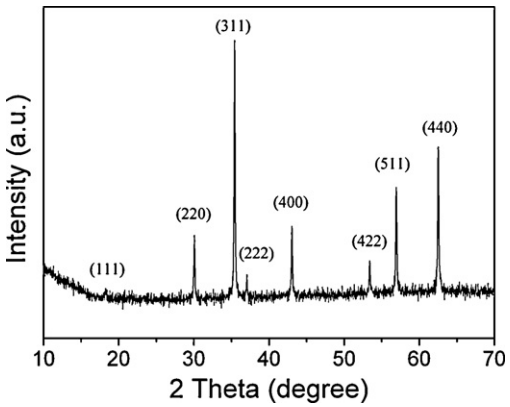

Fig. 1. XRD pattern of the powder prepared at 200 °C for 48 h.

microscopy (XL30 FEG) and transmission electron microscopy (PHILIPS TECNAI 12). Its composition was identified as Fe_3O_4 (see below). To evaluate the electrochemical properties of the Fe_3O_4 sample, a magnetite-based composite electrode consisting of Fe_3O_4 (40 wt%, as active material), acetylene black (30 wt%, Xinda Chemical, China Jiaozuo, as conducting additive) and poly-vinylidene difluoride (PVdF from Shenzhen Lexel Battery Co., 30 wt%, as binder) was made on copper foil by a tape-casting technique. Coin-type cells (2032) of Li/1 M $LiPF_6$ in ethylene carbonate and diethyl carbonate (EC-DEC, 1:1, v/v)/Fe_3O_4 were assembled in an argon-filled glove box (MBRAUN LAB MASTER130) where both moisture and oxygen levels were less than 1 ppm. A Celgard 2400 microporous polypropylene membrane was used as the separator. The cells thus fabricated were cycled galvanostatically in the voltage range between 0.01 and 3.0 V at a current of 0.31 mA with a multichannel battery test system (NEWARE BTS-610). To evaluate the rate performance, the cycling current was raised up to 10 mA. At the end of discharge in some cycles, the impedance spectra of the cells were measured on an electrochemical workstation (CHI 660A) in the frequency range of 0.005–100 kHz.

3. Results and discussion

Fig. 1 shows the XRD pattern of the sample prepared at 200 °C for 48 h. According to the JCPDS file (card no. 85-1436), a pure phase of Fe_3O_4 with high crystallinity is obtained. The SEM images of this powder are shown in Fig. 2a. It can be seen that the powder is composed of well-dispersed spheroids with a narrow particle size distribution in the range of 200–300 nm (inset of Fig. 2a). Under higher magnifications, we can clearly see that the spheroids are actually assembly of many nanospheres with diameter of about 30 nm. Such a microstructure provides a high surface area, which is desirable for an electrode material. The TEM image of the powder (Fig. 2b) also confirms the micro-assembly structure. In fact, some small spheres have been broken off from a large spherical assembly after the ultrasonic process.

The as-prepared sample is used as anode material for lithium-ion batteries to test the electrochemical performance (Fig. 3). Fig. 3a shows the voltage profiles for the first three cycles of the Fe_3O_4/Li cell. In the first discharge, there is a steep voltage drop from 3 to 0.75 V, which can be attributed to the reaction of $Fe_3O_4 + xLi \rightarrow Li_xFe_3O_4$. An obvious voltage plateau at 0.75 V corresponds to the conversion reaction $Li_xFe_3O_4 + (8-x)Li \rightarrow 3Fe + 4Li_2O$. The sloping part of the discharge curve between 0.7 and 0 V can be attributed to the reaction process of Fe and electrolyte to form a gel-like film and SEI film [15]. After the first cycle, the voltage plateau is not so obvious, and it seems to have changed into two slopes at 1.6–0.8 and 0.8–0 V. The Fe_3O_4 electrodes exhibit high capacity in the first cycle, which can deliver 1332 mAh g^{-1} in the first discharge process and 933 mAh g^{-1} in the first charge process. At the 60th cycle, the voltage profile and the specific capacity do not change so much compared with the initial cycles, indicating that the cycleability of the Fe_3O_4/Li cell is very good. The cycling performance of the Fe_3O_4/Li cell is shown in the inset of Fig. 3a. The capacity is stable without any capacity fading up to 60th cycle. After subtracting the contribution from carbon black [16,17], the reversible capacity contributed by the Fe_3O_4 spheres is around 840 mAh g^{-1}. Besides the high capacity, the rate capability is also very important for high performance lithium-ion batteries. The Fe_3O_4 electrodes show rather good rate capability with an average discharge-capacity of 1000 mAh g^{-1} at the current of 0.2 mA (1/7 C) (with the 2nd-cycle capacity of 1038 mAh g^{-1}), 560 mAh g^{-1} at the current of 4 mA (3.5 C rate), 410 mAh g^{-1} at 10 mA (7 C rate) (Fig. 3b). All of these values are higher than the theoretical capacity of the commonly used graphite electrode (372 mAh g^{-1}). And after large charge/discharge current, the capacity can go back to more than 900 mAh g^{-1} when the current is reduced to 0.31 and 0.2 mA. To our knowledge, Fe_3O_4 synthesized in this experiment shows better *C*-rate retention and cycling capability than before reported [10–14]. The enhanced cycling performance and rate capability are due to the unique structure of the sample which combines the benefit of nanostructure with high electrochemical activity and stable submicron sphere during the cycling. Also the high capacity achieved at a high cycling rate implies that this type of electrodes can be a promising candidate for high power applications.

Since the rate capability is directly related to the impedance of the cells, the impedance spectra of Fe_3O_4/Li cells at the end of the discharge in some cycles (1st, 10th, 30th, 60th) during 0.2 C

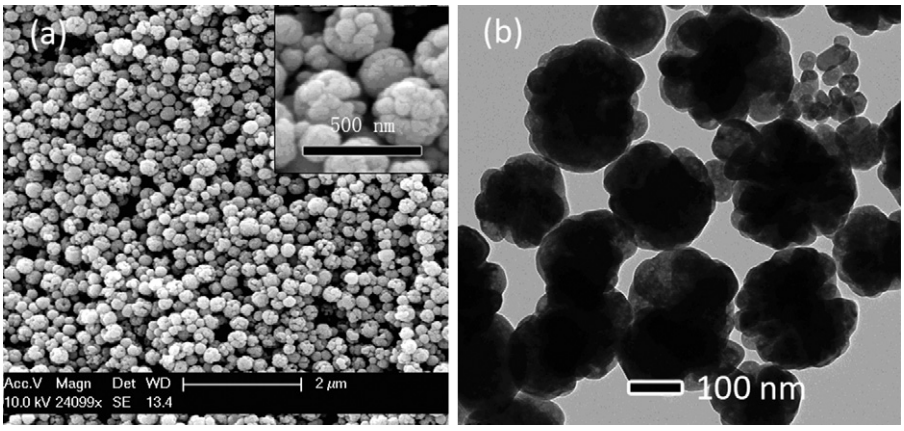

Fig. 2. The particle morphology of Fe_3O_4 microspheres: (a) SEM images and (b) TEM image.

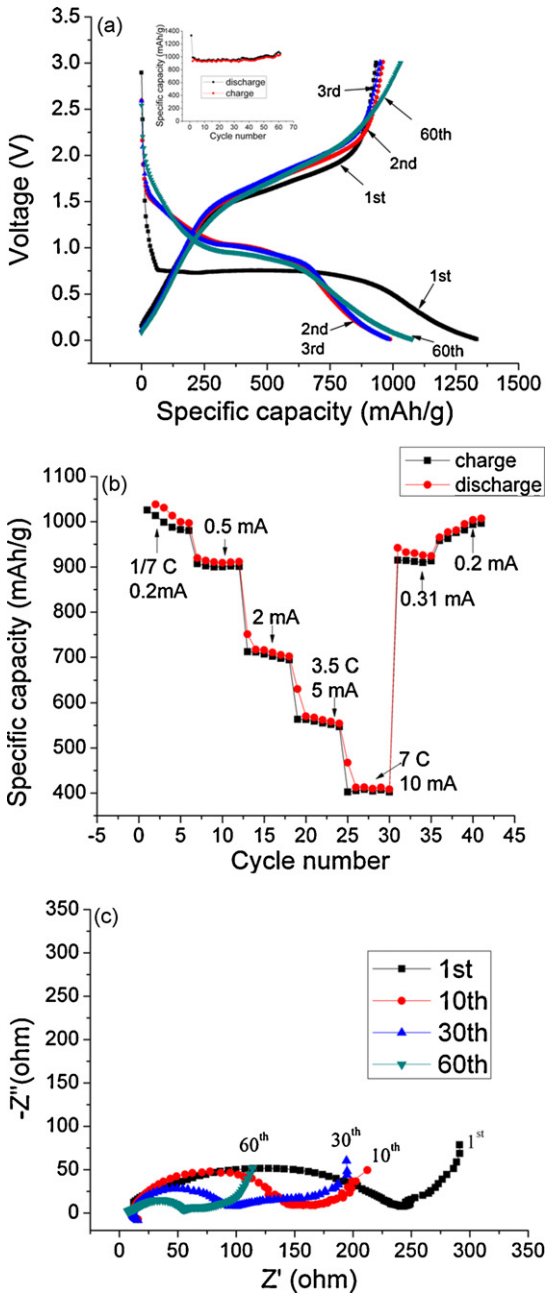

Fig. 3. Electrochemical performance of the Fe_3O_4/Li cells: (a) the voltage profiles at the current of 0.2 C rate; inset is the cycling performance at 0.2 C rate (*C*/*n* being defined as the rate for a cell to be fully charged or discharged in n hours); (b) the specific capacity of Fe_3O_4 electrode as a function of the cycling rate (0.2–10 mA); (c) impedance spectra at the open-circuit voltage of 0.01 V after some electrochemical cycles. Cycle numbers are indicated in the graph.

cycling (corresponding to Fig. 3a) are shown in Fig. 3c. The plots are similar to each other in shape, with one big depressed semicircle and one small semicircle appearing in the high frequency domain and a straight line in the low frequency region. It is clear that after 60 cycles, the cell impedance decreases substantially compared to its initial cycles. This change is likely due to the so-called electrochemical milling effect we reported before [18]. When the electrochemical milling occurs, the particles will become smaller. This pulverization process will increase the total surface area of the electrode material so that the contact area between the active material and electrolyte will largely increase. As a result, the cell impedance decreases as observed in Fig. 3c. In fact, similar results have been observed in a number of other metal oxides systems, for example, in Cu_2O–Li_2O composite electrode [19]. That is also why the good rate capability is obtained for this Fe_3O_4 electrode.

4. Conclusions

A low-temperature hydrothermal method can be used to synthesize Fe_3O_4 magnetite submicron spheroids with a narrow particle size distribution. The electrode made of the Fe_3O_4 powder has excellent electrochemical performance with a stable and reversible capacity of over 900 mAh g^{-1} and good rate capability. The unique nanostructure of the Fe_3O_4 particles can offer high capacity and improved cyclic stability because of the high interfacial contact area with the electrolyte and better accommodation of volume change. It is a promising anode material for high energy-density or high power lithium-ion batteries.

Acknowledgments

This study was supported by National Science Foundation of China (grant nos. 20971117 and 10979049) and Education Department of Anhui Province (grant no. KJ2009A142). We are also grateful to the Solar Energy Operation Plan of Academia Sinica.

References

[1] P. Poizot, S. Laruelle, S. Grugeon, L. Dupont, J.M. Tarascon, Nature 407 (2000) 496.
[2] H. Zeng, J. Li, J.P. Liu, Z.L. Wang, S.H. Sun, Nature 420 (2002) 395.
[3] F.Q. Hu, L. Wei, Z. Zhou, Y.L. Ran, Z. Li, M.Y. Gao, Adv. Mater. 18 (2006) 2553.
[4] H. Li, P. Balaya, J. Maier, J. Electrochem. Soc. 151 (2004) A1878.
[5] Y. Yu, C.H. Chen, J.L. Shui, S. Xie, Angew. Chem. Int. Ed. 44 (2005) 7085.
[6] H. Liu, G.X. Wang, J.Z. Wang, D. Wexler, Electrochem. Commun. 10 (2008) 1879.
[7] P.L. Taberna, S. Mitra, P. Poizot, P. Simon, J.-M. Tarascon, Nat. Mater. 5 (2006) 567.
[8] H.N. Duan, J. Gnanaraj, X.P. Chen, B.Q. Li, J.Y. Liang, J. Power Sources 185 (2008) 512.
[9] S. Ito, K. Nakaoka, M. Kawamura, K. Ui, K. Fujimoto, N. Koura, J. Power Sources 146 (2005) 319.
[10] Z.M. Cui, L.Y. Jiang, W.G. Song, Y.G. Guo, Chem. Mater. 21 (2009) 1162.
[11] W.M. Zhang, X.L. Wu, J.S. Hu, Y.G. Guo, L.J. Wan, Adv. Funct. Mater. 18 (2008) 3941.
[12] G.H. Lee, J.G. Park, Y.M. Sung, K.Y. Chung, W.I. Cho, D.W. Kim, Nanotechnology 20 (2009) 295205.
[13] L. Wang, Y. Yu, P.C. Chen, D.W. Zhang, C.H. Chen, J. Power Sources 183 (2008) 717.
[14] H. Deng, X.L. Li, Q. Peng, X. Wang, J.P. Chen, Y.D. Li, Angew. Chem. Int. Ed. 44 (2005) 2782.
[15] S. Laruelle, S. Grugeon, P. Poizot, M. Dolle, L. Dupont, J.-M. Tarascon, J. Electrochem. Soc. 149 (2002) A627.
[16] J.L. Shui, S.L. Zhang, W.L. Liu, Y. Yu, G.S. Jiang, S. Xie, C.F. Zhu, C.H. Chen, Electrochem. Commun. 6 (2004) 33.
[17] S.Q. Wang, J.Y. Zhang, C.H. Chen, Scripta Mater. 57 (2007) 337.
[18] D.W. Zhang, C.H. Chen, J. Zhang, F. Ren, Chem. Mater. 17 (2005) 5242.
[19] Y. Yu, Y. Shi, C.H. Chen, Nanotechnology 18 (2007) 0557062.